Self-Trapping and Anomalous Dispersion of DNA in Electrophoresis

Jaan Noolandi, Jean Rousseau, and Gary W. Slater
Xerox Research Center of Canada, Mississauga, Ontario, Canada L5K 2L1

and

Chantal Turmel and Marc Lalande
Institut de Recherche en Biotechnologie, Conseil National de Recherches du Canada, Montréal, Québec, Canada H4P 2R2

(Received 27 January 1987)

We present a high-field biased reptation model of gel electrophoresis. It is predicted that during their migration, DNA fragments can get trapped for long periods of time in near-zero-velocity, looplike compact conformations. As a consequence, the electrophoretic mobility of DNA is found to be a nonmonotonic function of the fragment size. We present experimental results showing this unique and unexpected consequence of anomalous dispersion due to DNA self-trapping in compact states.

PACS numbers: 36.20.Ey, 82.45.+z, 87.15.−v

The electrophoretic mobility μ of a DNA fragment is determined by its contour length S, its shape, and its electric charge, as well as by the conditions of the (gel) electrophoresis experiment. It is widely believed that the empirical relation $\mu \propto 1/S$, observed for moderately large fragments in the limit of zero electric field,[1] is an indication that migration occurs by reptation, i.e., the molecule goes head first through the obstacles of the gel. The first models showed that a field-driven snakelike motion does indeed lead to a $\mu \propto 1/S$ law.[2,3]

For large fragments and finite electric fields, μ becomes field dependent, but its dependence upon S decreases as the molecule stretches (the charge per unit length of the DNA is then the only relevant parameter), making electrophoretic separation of DNA very difficult.[4] A biased reptation model showed that these effects are due to a net stretching of the average molecular conformation in the field direction.[5,6]

In this paper, we generalize the Slater and Noolandi[5] (SN) model to long DNA fragments and high electric fields. A computer simulation for this model predicts that the fragments stop migrating during long intervals of time because they get "trapped" in long-lived, looplike, compact conformations. These very stable conformations do not contribute to chain motion because, contrary to the situation in a solution, only the total integrated longitudinal electric force acting on the molecule leads to chain motion in a gel; in the case of a loop conformation, this force is zero. As a consequence of this self-trapping, the mobility μ can become minimum for fragments of finite size. Finally, we report the results of a series of experiments showing a minimum mobility for intermediate size fragments in large fields, in agreement with our model.

In the biased reptation model,[5] the chain is considered trapped in a tube (formed by the obstacles of the gel) which allows only one-dimensional motion along the tube axis. The effective (primitive) chain is made of N segments of length a (the average pore size). The (one-dimensional) motion of the chain is seen as a series of forward (+) or backward (−) jumps in the tube, each of length a, time duration $\Delta t_{\pm}$, and probabilities $p_{\pm}$.

Without an electric field, we have $p_{\pm} = \frac{1}{2}$, i.e., pure Brownian motion, and $\Delta t_{\pm} = \tau_B = a^2/2D = a^2\xi/2k_BT \sim N$, where D and ξ are the diffusion constant and friction coefficient of the chain in its tube (the Einstein relation gives $\xi D = k_BT$).

With an electric field $\mathbf{E} = E\hat{\mathbf{x}}$, the DNA chain has an instantaneous longitudinal electric drift velocity (along the tube axis) $v_l(t)$ and an average electrophoretic mobility μ given by[3,5,6]

$$v_l(t) = QEh_x(t)/L\xi, \quad \mu = 3\mu_0\langle h_x^2\rangle/L^2,$$

where Q is the total charge of the chain and $L = Na$ is the length of its "tube," and $\mu_0 = Q/3\xi$ is a measure of the friction coefficient per unit charge of DNA. Finally, $h_x(t)$ is the instantaneous end-to-end distance of the tube in the field direction, while $\langle h_x^2\rangle$ is averaged over the duration of the migration. The velocity v_l *and* the Brownian motion (with diffusion constant D) are both responsible for chain motion.

With each jump, an end segment leaves the tube to create a new tube section. While this end segment goes in a random direction at $E = 0$, it tends to align in the field direction when $E \neq 0$ because it has an electric charge $q = Q/N$. If we assume that the projection x_1 of this segment on the field axis (with $-a \leq x_1 \leq a$) follows a Boltzmann distribution taking into account the electrostatic energy $\frac{1}{2}qEx_1$ of the segment, we find that[5]

$$\langle x_1\rangle/a = \coth\Theta - 1/\Theta \approx \Theta/3 + \cdots, \tag{1}$$

where $\Theta = qEa/2k_BT$ is the scaled electric field.

The SN model[5] assumes that $p_{\pm} = \frac{1}{2}(1 \pm \delta)$ and

$\Delta t_\pm = \tau_B$, with the bias $\delta = v_l \tau_B / a$ *chosen* to recover the correct longitudinal velocity $a(p_+ - p_-)/\tau_B = v_l$. Therefore, the main hypothesis here is that the field-driven bias δ modifies the probabilities $p_\pm$ to first order, but the times $\Delta t_\pm$ only to second (or higher) order. Clearly, this model is limited to $|\delta| < 1$, i.e., to small electric fields.

To generalize the SN model, we map the motion of DNA during a jump with the motion of a particle between two absorbing walls.[6] The chain moves in its tube in response to the Brownian motion and the drift velocity v_l; a "jump" of length $\pm a$ is the completion of a displacement of length $\pm a$ of the chain in its tube. This is similar to the problem of a particle midway between two absorbing walls at $r = \pm a$, with the particle having a diffusion constant D and a constant velocity v_l. We assume that $v_l(h_x)$ remains constant during the jump; $v_l(h_x)$ is fixed by the value of h_x for the conformation present before the jump, and it takes a new value only after the jump is completed.

From Eq. (6.15) in Feller,[7] which treats the problem of a particle between two absorbing walls, it is straightforward to show that the probabilities $p_\pm$ and the average first-passage times $\Delta t_\pm$ at distances $\pm a$ are given by

$$\Delta t_\pm(h_x) = \tanh[\delta(h_x)]\,\tau_B/\delta h_x, \tag{2}$$

$$p_\pm(h_x) = \{1 + \exp[\mp 2\delta(h_x)]\}^{-1}, \tag{3}$$

with $\tau_B = a^2/2D$ and $\delta = v_l \tau_B / a$. The low-bias limit ($|\delta| \ll 1$) gives $\Delta t_\pm \approx \tau_B[1 - \frac{1}{3}\delta^2 + \cdots]$ and $p_\pm(h_x) \approx \frac{1}{2}[1 \pm \delta + \ldots]$, in agreement with the SN model to first order in $|\delta|$. The high bias limit ($|\delta| \gg 1$), on the other hand, gives $\Delta t_\pm \approx \tau_B/|\delta| = a/|v_l|$ and probabilities $p_\pm$ rapidly converging to [1,0] (jumps biased towards a single end segment), typical of a simple drift regime where Brownian motion is negligible. In conclusion, the main effect of small biases is to modify the probabilities $p_\pm$ (to first order in δ), while large $|\delta|$'s fully bias the jumps *and* reduce their time duration $\Delta t_\pm$.

Equations (2) and (3) include the Brownian motion of the chain and give the correct longitudinal velocity $v_l = [p_+ - p_-]a/\Delta t_\pm = a\delta/\tau_B$.

We used the following procedure: After each jump of length $\pm a$ along the tube axis, the value of $\delta(h_x)$ is computed and used in Eqs. (2) and (3) to evaluate $\Delta t_\pm(\delta)$ and $p_\pm(\delta)$ for the next jump. A randomly chosen end segment (with probability $p_\pm$) then leaves the tube and goes in a random direction satisfying[5] Eq. (1), while the others follow within the tube. At time zero, the chains start with random-walk conformations.

The mobility is estimated after completion of 10^{5-7} jumps for each chain, i.e., after the chains have disengaged completely from their tube at least 10^3 times. The scaled mobility μ/μ_0 is calculated from the total displacement d (measured in units of a) of the center of mass of the chain (in the field direction) during these jumps, and the total time duration of the jumps $\sum \Delta t_\pm$ (measured in units of $\tau_B^1 = \tau_B/N$): $\mu/\mu_0 = 3(d/a)/[N\Theta\sum(\Delta t_\pm/\tau_B)]$.

Figure 1 shows μ/μ_0 as a function of the number of segments N of the primitive chain for some experimentally relevant scaled electric fields Θ. The curves show a clear minimum for $\Theta > 0.20$, with an asymptotic behavior for large fragments.

In Fig. 2, the displacement d/a is plotted as a function of time. For the small four-segment fragment, we have a high and rapidly fluctuating velocity. The eight-segment fragment shows some effect as its velocity drops down to low values for relatively long periods. For these two fragments, the thermal motion is strong enough to

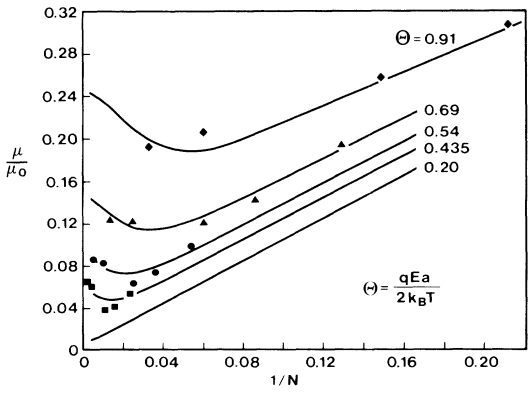

FIG. 1. Relative mobility μ/μ_0 as a function of $1/N$, for different values of the scaled electric field Θ. The lines follow the result of computer simulations. The points gives the mobilities of the fragments on Fig. 3, with $\mu_0 = 2.5 \times 10^{-4}$ cm^2/V·sec, and $A = 2.0\%$, $\langle s(a)\rangle = 0.10$ kbp/pore (squares); $A = 1.6\%$, $\langle s(a)\rangle = 0.24$ kbp (circles); $A = 1.2\%$, $\langle s(a)\rangle = 0.57$ kbp (triangles); $A = 0.8\%$, $\langle a(s)\rangle = 1.4$ kbp (lozenges).

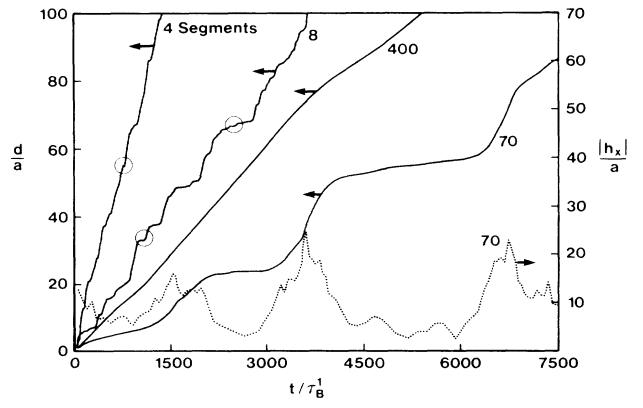

FIG. 2. Center-of-mass displacement d/a (solid lines) and end-to-end distance $|h_x|/a$ (dotted line) as a function of scaled time t/τ_B^1 (where $\tau_B^1 = \tau_B/N$ is the Brownian time per chain segment), for different values of N and $\Theta = 0.50$. In the circled regions, the chains go backward.

trigger jumps opposite to the field (circled).

The instantaneous center-of-mass velocity $V_x(t)$, velocity of the chain along its tube axis $v_l(t)$, and end-to-end distance $h_x(t)$, are related by $V_x(t)=v_l(t)h_x(t)/L=[a\delta(t)/\tau_B]h_x(t)/L$. Therefore, the low-velocity periods are related to conformations where $h_x\delta\propto h_x^2$ is small, i.e., to looplike conformations where both ends are close to each other in the field direction.[8] Similarly, high-velocity periods are related to extended conformations ($h_x^2\approx L^2$). This correlation is clearly seen in Fig. 2 for the seventy-segment fragment, the velocity of this fragment is almost zero for the very long periods, and the dotted curve shows that the fragment is then in a looplike state, with both ends close to each other.[8]

The probability that the motion of the chain through the gel leads to a looplike state is decreasing (exponentially) with N, as for long chains this necessitates a large number of consecutive unfavorable orientations of the end segments against the field direction; in Fig. 2 for example, the number of plateaus decreases very quickly for larger N's.

According to Eq. (2), jump times $\Delta t_\pm$ decrease with increasing $\delta\propto h_x$; looplike conformations ($h_x\rightarrow 0$) are therefore more stable (or long lived) than extended ones, as the time that it takes to make a jump from the former ($\approx\tau_B$) is longer than for the latter ($\approx\tau_B/|\delta|$, with $|\delta|\gg 1$). For extended conformations, the drift along the tube axis leads to fast changes. However, the total longitudinal electric force acting on a looplike conformation is negligible; slow unbiased reptation is then the only mechanism leading to conformation changes. Moreover, since $\tau_B\propto N$, the lifetime of the looplike states increase (algebraically) with the size of the fragment; in Fig. 2, the lifetime of the zero-velocity looplike states is indeed very long for $N=70$.

These looplike states therefore act as traps, more likely to happen for smaller fragments, but more stable for longer ones. For small fragments, $\Delta t_\pm\approx\tau_B$ as $|\delta|\propto N$ is always small, and although the fragments get trapped very easily, the net effect is small (Fig. 2). For very long fragments, the effect of the looplike states is reduced by their small probability of occurrence. It is for intermediate fragments ($N=70$ in Fig. 2) that both the probability of getting trapped and the relative lifetimes of the looplike states are large; consequently, it is for these fragments that the average mobility is the lowest.

In conclusion, intermediate-size fragments can get trapped in slow-moving long-lived compact (or looplike) states which reduce their average mobility as compared to both short fragments (for which all states are relatively short lived) and long fragments (for which a compact state is highly improbable).

Gel electrophoresis of DNA fragments ranging in size from 4.4 to 41.7 kilobase pairs (kbp) was performed in (0.8–2.0)% agarose gels with electric fields between 0.3 and 2.3 V/cm (see legend of Fig. 3 for details). Our model predicts a nonmonotonic mobility-fragment size relation for $\Theta>0.2$ and $N>10$–50; since $\Theta\propto E$, it is clear that higher fields are to be preferred. However, while the number of segments N of a given chain is inversely proportional to the average pore size a, $\Theta\propto qa$ is directly proportional to a. Therefore, the choice of the agarose concentration A (in percent) is critical: Low A's would give too small N's, while large A's would lead to too small Θ's.

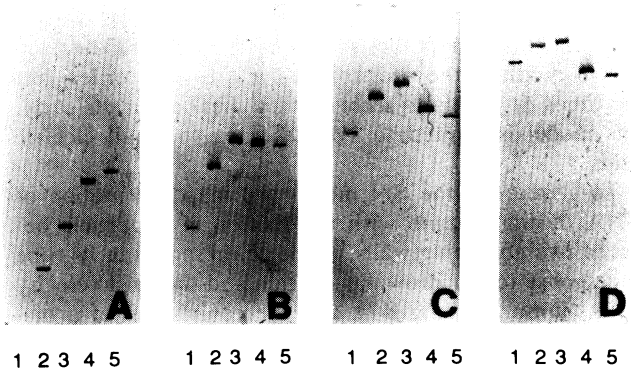

FIG. 3. Phage lambda/DNA Hind III fragments of 4.4 kbp (lane 1), 6.6 kbp (lane 2), 9.4 kbp (lane 3), and 23.1 kbp (lane 4) fragments were separated by electrophoresis at 1 V/cm in 0.8% weight/volume agarose gels. The DNA fragments were recovered from the gels by electroelution into dialysis bags (Ref. 9). The lambda/DNA Hind III fragments have been calibrated (Ref. 10) in terms of fragment size vs mobility in agarose gels of approximately 1.0%. The 41.7-kbp (lane 5) fragment is a monomeric DNA molecule isolated from the lambda phage Charon 21A by standard procedures (Ref. 9). Agarose (type NA, Lot MH02661, Pharmacia, Uppsala, Sweden) was dissolved by boiling in the electrophoresis buffer [89 mM tris base, 89 mM boric acid, 2 mM ethylenediamine tetra-acetic acid (EDTA)]. After cooling to 60 °C, 100 ml of agarose solution at concentrations of $A=0.8\%$ (panel A), 1.2% (B), 1.6% (C), or 2.0% (D) was poured into a (11×14)-cm gel bed on which a 14-well gel slot former was mounted. The slots were 2×4.8 mm in width. After solidification, the gel was submerged in 900 ml of electrophoresis buffer to a depth of 4 mm above the gel surface. The DNA samples were resuspended in a loading buffer (Ref. 11) and added to separate slots. Downward electrophopresis was performed for 16 h (panel A) or 22 h (B–D) in a horizontal gel electrophoresis apparatus (Model H3, Bethesda Research Laboratories, Gaithersburg, Maryland) at 2.4 V/cm with use of a commercial constant voltage output power supply. The electrophoresed DNA was stained with the fluorescent dye ethedium bromide (1 μg/ml), visualized with an ultraviolet transilluminator (Model T5-15, Ultra-Violet Products, San Gabriel, California) and photographed with a standard gel photography apparatus. Measurements of migration distances were made directly from the photographs of the gels.

Figure 3 shows examples from a series of gel electrophoresis carried out for different agarose concentrations

A with $E=2.3$ V/cm. The effect predicted in the previous section is seen, as the 9.4-kbp fragment has the lowest mobility for $A \geq 1.2\%$.

We also carried out experiments where the field was varied at $A=1.5\%$ (not shown here). While the 23.1-kbp fragment was found to have the minimum mobility at $E=0.65$ V/cm, the 9.4-kbp fragment had the minimum mobility at $E=1.94$ V/cm, and both fragments had approximately the same mobility at $E=0.97$ V/cm.

The mobilities measured in Fig. 3 are shown in Fig. 1 for comparison; we have used $\mu_0=2.5\times10^{-4}$ cm^2/V·sec, as obtained from previous experiments,[11] to scale the mobilities. The lines on Fig. 1 represent the best fits obtained by the use of two parameters: the scaled electric field Θ and the value of $\langle s(a)\rangle=S/N$, which acts as a scaling factor between the length S of the fragments and the corresponding number of segments N. Good agreement is obtained with reasonable values for these parameters.

It is remarkable that such an important effect has been overlooked up to now considering the extreme importance of gel electrophoresis in today's biotechnology. This effect has been reported in the case of field-inversion gel electrophoresis, but was interpreted as an artifact of the method.[12] Our results show that band inversion is a natural phenomena bound to happen in any condition where the field and the agarose concentration are such that both N and Θ are large for the fragments used. These conditions are, in fact, typical working conditions.

Possibly, results of many previous electrophoresis experiments have been wrongly interpreted by the inability to identify the bands in the right order. Our own experience tells us that band inversion can be reduced or even eliminated by a correct but delicate choice of electric field pulses, and that the effect generally occurs under most conditions of pulsed fields.[13]

We would like to thank L. M. Marks for helping us with the computer program. One of us (G.W.S.) acknowledges receipt of an Industrial Research Fellowship from the Natural Sciences and Engineering Research Council of Canada. This work has been supported by the National Research Council of Canada.

[1]S. P. Edmondson and D. M. Gray, Biopolymers **23**, 2725 (1984).

[2]L. S. Lerman and H. L. Frisch, Biopolymers **21**, 995 (1982).

[3]O. J. Lumpkin and B. H. Zimm, Biopolymers **21**, 2315 (1982).

[4]W. L. Fangman, Nucleic Acids Res. **5**, 653 (1978).

[5]G. W. Slater and J. Noolandi, Biopolymers **25**, 431 (1986).

[6]G. W. Slater, J. Rousseau, and J. Noolandi, Biopolymers (to be published).

[7]W. Feller, *An Introduction to Probability Theory and Its Applications* (Wiley, New York, 1968), Vol. 1, p. 359.

[8]Note that the ends of the chain are close to each other only in the field direction; the field does reduce the distance between the ends in the other directions, but this is a second-order effect [G. W. Slater and J. Noolandi, Macromolecules **19**, 2356 (1986)]. Therefore, the expressions "looplike" and "compact" used here refer solely to the field (x) direction.

[9]T. Maniatis, E. S. Fritsch, and J. Sambrook, *Molecular Cloning: A Laboratory Manual* (Cold Spring Harbor Laboratory, New York, 1982).

[10]L. H. Robinson and A. Landy, Gene **2**, 1 (1977).

[11]G. W. Slater, J. Rousseau, J. Noolandi, C. Turmel, and M. Lalande, to be published.

[12]G. F. Carle, M. Frank, and M. V. Olson, Science **232**, 65 (1986).

[13]M. Lalande, J. Noolandi, G. W. Slater, C. Turmel, C. Collins, and J. Rousseau, to be published.

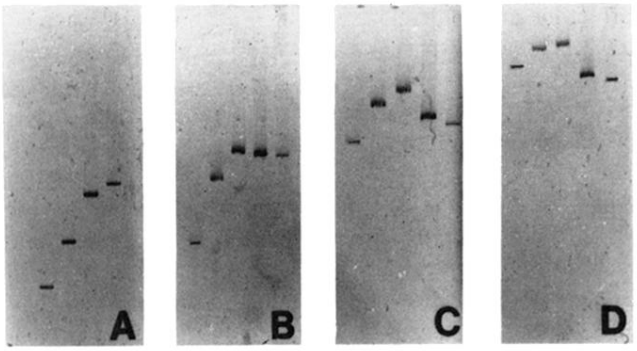

FIG. 3. Phage lambda/DNA Hind III fragments of 4.4 kbp (lane 1), 6.6 kbp (lane 2), 9.4 kbp (lane 3), and 23.1 kbp (lane 4) fragments were separated by electrophoresis at 1 V/cm in 0.8% weight/volume agarose gels. The DNA fragments were recovered from the gels by electroelution into dialysis bags (Ref. 9). The lambda/DNA Hind III fragments have been calibrated (Ref. 10) in terms of fragment size vs mobility in agarose gels of approximately 1.0%. The 41.7-kbp (lane 5) fragment is a monomeric DNA molecule isolated from the lambda phage Charon 21A by standard procedures (Ref. 9). Agarose (type NA, Lot MH02661, Pharmacia, Uppsala, Sweden) was dissolved by boiling in the electrophoresis buffer [89 mM tris base, 89 mM boric acid, 2 mM ethylenediamine tetra-acetic acid (EDTA)]. After cooling to 60 °C, 100 ml of agarose solution at concentrations of $A = 0.8\%$ (panel A), 1.2% (B), 1.6% (C), or 2.0% (D) was poured into a (11×14)-cm gel bed on which a 14-well gel slot former was mounted. The slots were 2×4.8 mm in width. After solidification, the gel was submerged in 900 ml of electrophoresis buffer to a depth of 4 mm above the gel surface. The DNA samples were resuspended in a loading buffer (Ref. 11) and added to separate slots. Downward electrophopresis was performed for 16 h (panel A) or 22 h (B–D) in a horizontal gel electrophoresis apparatus (Model H3, Bethesda Research Laboratories, Gaithersburg, Maryland) at 2.4 V/cm with use of a commercial constant voltage output power supply. The electrophoresed DNA was stained with the fluorescent dye ethedium bromide (1 μg/ml), visualized with an ultraviolet transilluminator (Model T5-15, Ultra-Violet Products, San Gabriel, California) and photographed with a standard gel photography apparatus. Measurements of migration distances were made directly from the photographs of the gels.